Hydrothermal synthesis of MoS_2 nanoflowers and their capacitive property

Qinghua Yang, Chunni Xiao, Bingbing Chen, Lin Ma ✉, *Limei Xu*

School of Chemistry and Chemical Engineering, Lingnan Normal University, Zhanjiang 524048, People's Republic of China
✉ *E-mail: ma_lin75@126.com*

Published in Micro & Nano Letters; Received on 30th October 2018; Revised on 27th December 2018; Accepted on 15th January 2019

MoS_2 hierarchical nanoflowers are fabricated through a gelatin-assisted hydrothermal route. The obtained MoS_2 products are characterised by X-ray powder diffraction, scanning electronic microscopy, transmission electronic microscopy and X-ray photoelectron spectra. It is indicated that MoS_2 nanoflowers (MoS_2 NFs) are assembled by nanosheets as building blocks and gelatin plays a crucial role in the formation of these novel structures. Moreover, MoS_2 NF electrode exhibits an enhanced capacitive property because of its unique microstructure.

1. Introduction: Enormous efforts have been made to explore suitable energy storage and conversion devices so as to satisfy the growing demand for energy and solve the energy crisis [1]. Up to now, rechargeable batteries, fuel cells as well as electrochemical capacitors that can realise conversion between chemical energy and electrical energy, have been proven as effective energy storage and conversion systems for practical applications [2]. Electrochemical supercapacitors are burgeoning promising energy storage devices for flexible electronics and electric vehicles because of their high power density, good pulse charge–discharge performance and long cycle life [3]. The capacitance of capacitors can be mainly caused by the surface reaction of electrode materials, such as the surface charge separation at the electrode/electrolyte interface (electrochemical double-layered capacitance) and surface Faradaic redox reaction (pseudocapacitance) [4]. Carbon materials usually exhibit electrochemical double-layered capacitive behaviour while transition metal oxides or conductive polymers manifest pseudocapacitive behaviour [5, 6].

Layered transition-metal chalcogenides, for example MoS_2, which are composed of metal layers and sulphur layers and stacked together by weak Van der Waals interactions, have been established as a new paradigm for energy storage for their unique physical and chemistry properties [7, 8]. Recently, MoS_2 has been investigated as a new type of supercapacitor material for its 2D sheet-like morphology which can provide a large surface area to enhance the double-layer charge storage. Moreover, Mo also displays variable valence states, which endows MoS_2 with pseudocapacitive properties [9, 10].

Nevertheless, separate MoS_2 nanosheets (MoS_2 NSs) are prone to overlap and aggregate, giving rise to a large loss of effective surface area. Additionally, serious volumetric expansion during repeated charge/discharge process can cause pulverisation of active materials and capacity fading [11, 12]. Fabricating hierarchical architecture has been proved to be a feasible strategy to solve these problems. It is widely believed that hierarchical micro/nanoarchitectures can combine the features of micrometre- and nanometre-scaled building blocks and show the unique properties different from those of the mono-morphological structures. For instance, hierarchical architectures can provide more electrode/electrolyte interface area, multi-level ions diffusion channels and more stable frameworks to withstand mechanical stress [13]. Until now, a variety of hierarchical MoS_2 architectures have been fabricated and demonstrated good electrochemical performances [14, 15]. Gelatin is the denaturation product of collagen, which is the major structural protein in the connective tissue of animal skin and bone. This protein is rather simple consisting of a highly repetitive sequence of amino acids $[(Gly)–X–Y]_n$, where Gly stands for glycine, X is often proline, and Y is hydroxyproline. Gelatin consists of a single chain of these sequenced amino acids and is promptly soluble in warm water [16]. It can form a homogeneous aqueous solution with high viscosity, widely used as a colloidal protecting agent, surfactant and thickening agent [17]. It has been reported that anionic gelatin (Type B) created by alkaline treatment has a high percentage of carboxylic groups. Thus the anionic gelatin has a negatively charged surface, which has a strong electrostatic attraction with metal ions to rapidly form precipitates [18]. However, the negative-charged feature of anionic gelatin is favourable for the homogeneous nucleation of MoS_2 because of electrostatic repulsion between anionic gelatin and MoO_4^{2-} ions before hydrothermal reaction. Moreover, gelatin is a strong cross-linker with multifunctional groups, which enables gelatin to interact with nanoparticles and direct the assembly of nanomaterials [16, 19, 20].

Here, a hydrothermal method is introduced to prepare hierarchical MoS_2nanoflowers (MoS_2 NFs) assembled by nanosheets with gelatin as a morphology-directing agent. In addition, their electrochemical properties are also investigated as an electrode for supercapacitor.

2. Experimental details: All chemical reagents were purchased from Aladdin Industrial Co. Ltd. (Shanghai, China). 3 mmol of sodium molybdate and 15 mmol of thiourea were dissolved in 60 ml water to form a clear solution. Then 1 g of gelatin (Type B, 250 bloom from porcine skin) was slowly dropped into the above solution under vigorous stirring. The resultant viscous solution was transferred into a Teflon-lined autoclave and heated at a rate of 5°C/min and maintained at 220°C for 24 h. Afterwards, the autoclave was cooled down naturally in air to room temperature. The black precipitates were collected, washed with water and alcohol, and dried at 60°C for 12 h in a vacuum oven to obtain MoS_2 NFs. For comparision, the MoS_2 NSs were also prepared via a similar route without gelatin.

The samples were characterised by X-ray diffraction (XRD) (D/Max-2550), field-emission scanning electron microscopy (FE-SEM) (FEI SIRION-100), transmission electron microscopy (TEM) (JEOL JEM-2010F) and X-ray photoelectron spectra (XPS) recorded on an ESCALAB 250. The nitrogen adsorption–desorption was conducted at 77 K on a Quantachrome NOVA 2000e sorption analyser (USA), and the Brunauer–Emmett–Teller (BET) surface area was estimated from the adsorption data. Electrochemical performance was measured by cyclic voltammetry (CV) and charge/discharge techniques on an electrochemical station (CHI660E). Na_2SO_4 solution (1 M) was electrolysed in a three-electrode cell. The sample-based electrode was the working electrode, platinum plate electrode as the counter electrode and the saturated calomel electrode as the reference electrode.

The active material (MoS_2 sample), carbon black (conductive agent) and polyvinylidene fluoride (binder) were blended at a mass ratio of 75:10:15 and were dispersed in N-methyl pyrrolidone to form a slurry by ultrasonic treatment. Then the slurry was pasted onto the nickle foam current collector (1 cm^2), dried at 60°C for 12 h and pressed to fabricate the working electrode. The scanning rate of the CV response varied from 5 to –100 mV/s with the potential window ranging from −0.8 to −0.2 V. The discharge capacitance values C at different current densities were calculated from the discharge curves based on equation $C = i\Delta t/\Delta V$, where C is called as the discharge capacitance; ΔV is the voltage range; i is the current density; Δt is the discharge time.

3. Results and discussions: The morphology and microstructure of the MoS_2 products are displayed in Fig. 1. It can be found that the MoS_2 products (MoS_2 NS) prepared without gelatin are scattered nanosheets (Fig. 1*a*). When gelatin is introduced, the obtained MoS_2 products (MoS_2 NF) are flower-like spheres with numerous curly nanosheets dispersed on the rough surfaces to form interconnected porous structures (Fig. 1*b*). The porous microstructures are presumed to provide a large contact surface with electrolyte and abundant pathways for ions transport. Fig. 1*c* also shows that many curly nanosheets stretch out of the edges of these nanoflowers. Owing to the rich functional groups and an 3D network of gelatin, the formation of the MoS_2 NF could be ascribed to a gelatin-induced assembly process [16, 17]. High-resolution TEM (HRTEM) image in Fig. 1*d* reveals that these nanosheets are composed of a few MoS_2 layers with an interlayer space of 0.64 nm corresponding to the *d*-spacing of (002) plane.

Fig. 2*a* provides the XRD patterns of the obtained MoS_2 products, from which all the diffraction peaks can be assigned to the 2H-MoS_2 phase (JCPDS Card No. 37-1492). Compared with MoS_2 NS, MoS_2 NF displays an obviously weakened peak of the (002) plane, which can be indicative of underdeveloped stacking layers along the *c*-axis owing to the inhibition effect of gelatin polymer networks [15]. The chemical and surface states of the MoS_2 NF were examined by XPS. It can be seen in Fig. 2*b* that three peaks at 228.9, 232.2 and 235.8 eV can be assigned to Mo^{4+}-$3d_{5/2}$, Mo^{4+}-$3d_{3/2}$ and Mo^{6+}, respectively [10, 12, 15]. The S-2p peaks at 161.7, 162.9 and 163.8 eV in Fig. 2*c* can be affiliated to S^{2-}-$2p_{3/2}$, S^{2-}-$2p_{1/2}$ and S_2^{2-}-$2p_{1/2}$, respectively [10, 12, 15]. The surface areas of the MoS_2 samples are determined by nitrogen

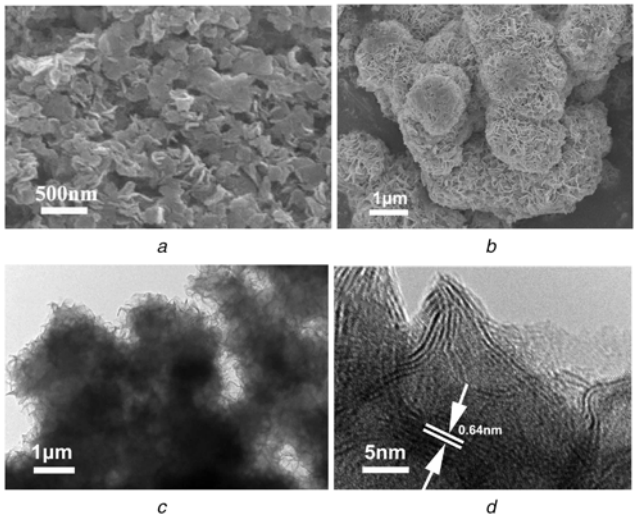

Fig. 1 *Images of*
a MoS_2 NS under SEM
b MoS_2 NF under SEM
c MoS_2 NF under TEM
d MoS_2 NF under HRTEM

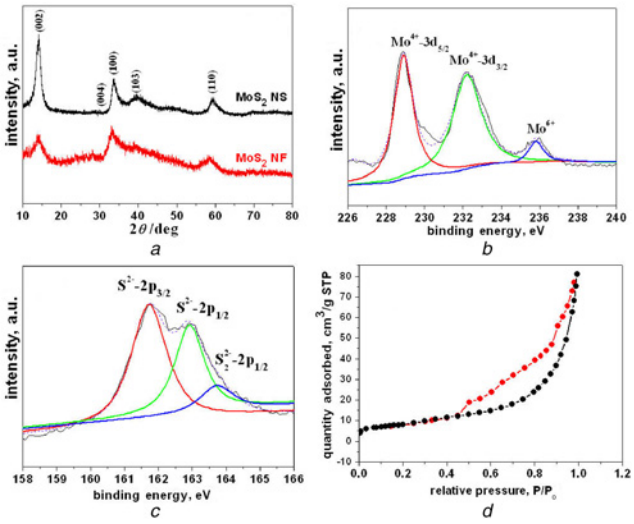

Fig. 2 *Phase, chemical state and pore type of the samples*
a XRD patterns
High-resolution XPS spectra of the MoS_2 NF of
b Mo-3d
c S-2p
d Nitrogen adsorption–desorption curves of MoS_2 NF

adsorption–desorption isotherm measurements. Fig. 2*d* shows a typical type IV with a hysteresis loop in the pressure range of 0.5–1.0 (P/P_0), revealing a mesoporous feature for MoS_2 NF. The BET surface area of the MoS_2 NF is measured to be 25.62 m^2g^{-1}, larger than that of the MoS_2 NS (9.13 m^2g^{-1}).

The electrochemical supercapacitor performance of the MoS_2 products was also measured. Figs. 3*a* and *b* depict the CV curves of MoS_2 NS and MoS_2 NF at various scan rates, respectively. The profiles of CV curves are different from the ideal rectangular curves of the electric double-layer capacitance, which confirms their pseudocapacitance features. With the scan rate increasing, the CV curves still maintain a similar shape except for a small shift of peak positions because of the electrode polarisation [10–15]. The areas below the CV curves become enlarged with increased scan rates, indicating that the MoS_2 electrodes demonstrate the ideal supercapacitive behaviour [10–15]. It is evident that the MoS_2 NF delivers a much higher capacitance than MoS_2 NS due to its larger CV curve area. In addition, there are no obvious redox peaks on the CV curves, which confirm that the capacitance of MoS_2 electrode may arise from electrosorption process at the MoS_2 surface [10–15]. The charge and discharge curves at different current densities are shown in Figs. 3*c* and *d*. The discharge-specific capacitance of MoS_2 NS is 105, 63, 38 and 22 Fg^{-1} at 1, 2, 4 and 10 Ag^{-1}, respectively. By contrast, MoS_2 NF demonstrates an enhanced capacitive performance. At 1, 2, 4 and 10 Ag^{-1}, the capacitance reaches to 220, 188, 145 and 103 Fg^{-1}, respectively.

Fig. 4*a* correlates the specific capacitance and current density. From 1 Ag^{-1} to 10 Ag^{-1}, MoS_2 NS electrode manifests a low-capacitance retention rate of ~21%, whereas MoS_2 NS electrode maintains a higher value of 47%, indicating a better rate capability than MoS_2 NS. Fig. 4*b* displays that after 2250 cycles, MoS_2 NF electrode still demonstrates a capacity of 141.57 Fg^{-1}, about retention rate of 97% according to its initial capacity of 145 Fg^{-1}, indicating a high cycling stability.

To further illustrate the enhanced electrochemical performance of MoS_2 NF electrode, the CV peak current density (i) relating to the scan rate (v) can be expressed by the equation ($i = av^b$). The value b shows the kind of charge storage occurring in the material, which is between 0.5 and 1. If $b = 0.5$, the current is controlled by the diffusion-controlled process; if $b = 1$, the current is controlled by

doi: 10.1049/mnl.2018.5665

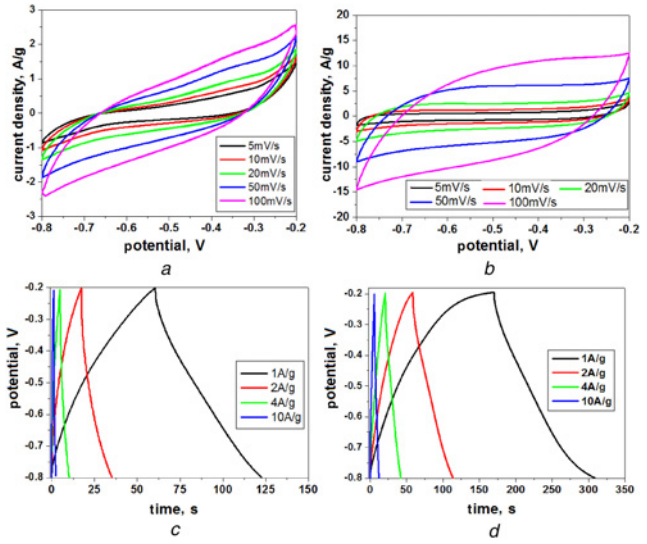

Fig. 3 *Cyclic voltammetry (CV) and chronopotentiometry measurements of the sample electrodes. CV of*
a MoS_2 NS
b MoS_2 NF
Charge/discharge curves at various current densities of
c MoS_2 NS
d MoS_2 NF

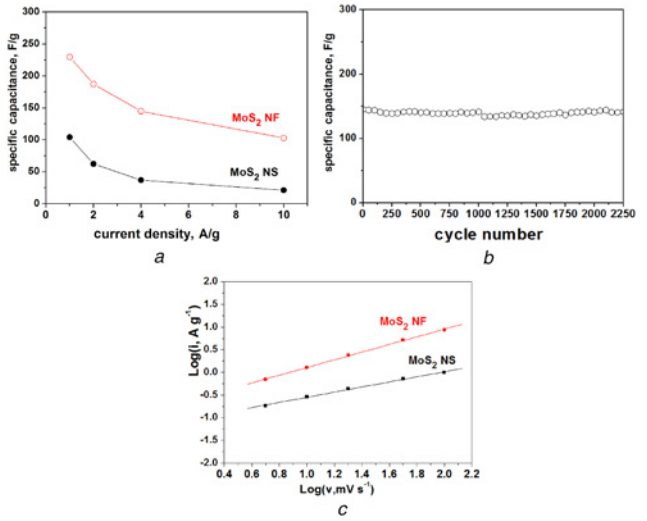

Fig. 4 *Rate capability, cycling performance and the kind of charge storage of the sample electrodes*
a Specific capacitances versus current densities
b Cycling stability of MoS_2 NF at 4 Ag^{-1}
c log *i* versus log *v* plots for obtaining *b* values

the surface-controlled process. The *b* value of MoS_2 NF can be estimated to be 0.85 larger than that of MoS_2 NS (0.56) in Fig. 4*c*, indicating that electrochemical reactions occurred in MoS_2 NF are surface controlled [21]. Therefore, MoS_2 NF displays enhanced capacitive behaviour and faster kinetics than MoS_2 NS.

4. Conclusion: In brief, a gelatin-assisted hydrothermal method has been developed to prepare hierarchical MoS_2 NFs assembled by nanosheets. The hierarchical architectures can afford large active surface area for electrode reactions, provide multi-level channels for charge carriers diffusion and effectively alleviate volume variation. The desirable structural merits along with the surface-dominated capacitive contribution of MoS_2 NF result in a superior electrochemical performance to the MoS_2 NS electrode.

5. Acknowledgments: The authors acknowledge financial funding from the Guangdong Natural Science Foundation (grant nos. 2017A030313074, 2016A030313667 and 2014A010106032), Training Plan to Innovation and Enterprise of Undergraduates of Guangdong Province (grant nos. 201610579384 and 201710579461).

6 References

[1] Zhu Y., Peng L.L., Fang Z.W., *ET AL.*: 'Structural engineering of 2D nanomaterials for energy storage and catalysis', *Adv. Mater.*, 2018, **30**, (15), p. 1706347
[2] Hu P.F., Chen T.H., Yang Y., *ET AL.*: 'Renewable-emodin-based wearable supercapacitors', *Nanoscale*, 2017, **9**, (4), pp. 1423–1427
[3] Shukla A.K., Banerjee A., Ravikumar M.K., *ET AL.*: 'Electrochemical capacitors: technical challenges and prognosis for future markets', *Electrochim. Acta*, 2012, **84**, pp. 165–173
[4] Fic K., Platek A., Piwek J., *ET AL.*: 'Sustainable materials for electrochemical capacitors', *Mater. Today*, 2018, **21**, (4), pp. 437–454
[5] Inagaki M., Konno H., Tanaike O.: 'Carbon materials for electrochemical capacitors', *J. Power Sources*, 2010, **195**, (24), pp. 7880–7903
[6] Chen D, Wang Q.F., Wang R.M., *ET AL.*: 'Ternary oxide nanostructured materials for supercapacitors: a review', *J. Mater. Chem. A*, 2015, **3**, (19), pp. 10158–10173
[7] Heine T.: 'Transition metal chalcogenides: ultrathin inorganic materials with tunable electronic properties', *Acc. Chem. Res.*, 2015, **48**, (1), pp. 65–72
[8] Eng A.Y.S., Ambrosi A., Sofer Z., *ET AL.*: 'Electrochemistry of transition metal dichalcogenides: strong dependence on the metal-to-chalcogen composition and exfoliation method', *ACS Nano*, 2014, **8**, (12), pp. 12185–12198
[9] Bissett M.A., Worrall S.D., Kinloch I.A., *ET AL.*: 'Comparison of two-dimensional transition metal dichalcogenides for electrochemical supercapacitors', *Electrochim. Acta*, 2016, **201**, pp. 30–37
[10] Pujari R.B., Lokhande A.C., Shelke A.R., *ET AL.*: 'Chemically deposited nano grain composed MoS_2 thin films for supercapacitor application', *J. Colloid Interface Sci.*, 2017, **496**, pp. 1–7
[11] Huang K.J., Wang L., Liu Y.J., *ET AL.*: 'Layered MoS_2–graphene composites for supercapacitor applications with enhanced capacitive performance', *Int. J. Hydrog. Energy*, 2013, **38**, (32), pp. 14027–14034
[12] Ji H.M., Liu C., Wang T., *ET AL.*: 'Porous hybrid composites of few-layer MoS_2 nanosheets embedded in a carbon matrix with an excellent supercapacitor electrode performance', *Small*, 2015, **11**, (48), pp. 6480–6490
[13] Yue Y., Liang H.: 'Hierarchical micro-architectures of electrodes for energy storage', *J. Power Sources*, 2015, **284**, pp. 435–445
[14] Gao Y.P., Huang K.J., Wu X., *ET AL.*: 'MoS_2 nanosheets assembling three-dimensional nanospheres for enhanced-performance supercapacitor', *J. Alloys Compd.*, 2018, **741**, pp. 174–181
[15] Chao J., Deng J.W., Zhou W.J., *ET AL.*: 'Hierarchical nanoflowers assembled from MoS_2/polyaniline sandwiched nanosheets for high-performance supercapacitors', *Electrochim. Acta*, 2017, **243**, pp. 98–104
[16] Bauermann L.P., del Campo A., Bill J., *ET AL.*: 'Heterogeneous nucleation of ZnO using gelatin as the organic matrix', *Chem. Mater.*, 2006, **18**, (8), pp. 2016–2020
[17] Thakur S., Govender P.P., Mamo M.A., *ET AL.*: 'Recent progress in gelatin hydrogel nanocomposites for water purification and beyond', *Vacuum*, 2017, **146**, pp. 396–408
[18] Zhou L., Tan G., Tan Y., *ET AL.*: 'Biomimetic mineralization of anionic gelatin hydrogels: effect of degree of methacrylation', *RSC Adv.*, 2014, **4**, (42), pp. 21997–22008
[19] Du H., Yuan C., Huang K., *ET AL.*: 'A novel gelatin-guided mesoporous bowknot-like Co_3O_4 anode material for high-performance lithium-ion batteries', *J. Mater. Chem. A*, 2017, **5**, (11), pp. 5342–5350
[20] Zhou X.J., Weng W.Z., Chen B., *ET AL.*: 'Mesoporous silica nanoparticles/gelatin porous composite scaffolds with localized and sustained release of vancomycin for treatment of infected bone defects', *J. Mater. Chem. B*, 2018, **6**, (5), pp. 740–752
[21] Li X., Li J.H., Gao Q.S., *ET AL.*: 'MoS_2 nanosheets with conformal carbon coating as stable anode materials for sodium-ion batteries', *Electrochim. Acta*, 2017, **254**, pp. 172–180